Viral myocarditis involves the generation of autoreactive T cells with multiple antigen specificities that localize in lymphoid and non-lymphoid organs in the mouse model of CVB3 infection

Rakesh H. Basavalingappa[a,1,2], Rajkumar Arumugam[a,1], Ninaad Lasrado[a,1], Bharathi Yalaka[b], Chandirasegaran Massilamany[c], Arunakumar Gangaplara[d], Jean-Jack Riethoven[e], Shi-Hua Xiang[a], David Steffen[a], Jay Reddy[a,*]

[a] School of Veterinary Medicine and Biomedical Sciences, University of Nebraska-Lincoln, Lincoln, NE, USA
[b] Bristol-Myers Squibb, Hopewell, Pennington, NJ, USA
[c] CRISPR Therapeutics, Cambridge, MA, USA
[d] Laboratory of Early Sickle Mortality Prevention, Cellular and Molecular Therapeutics Branch, National Heart, Lung, and Blood Institute, Bethesda, MD, USA
[e] Center for Biotechnology, University of Nebraska-Lincoln, Lincoln, NE, USA

ARTICLE INFO

ABSTRACT

Autoreactive T cells may contribute to post-viral myocarditis induced with Coxsackievirus B3 (CVB3), but the underlying mechanisms of their generation are unclear. Here, we have comprehensively analyzed the generation of antigen-specific, autoreactive T cells in the mouse model of CVB3 infection for antigens implicated in patients with myocarditis/dilated cardiomyopathy. First, comparative analysis of CVB3 proteome with five autoantigens led us to identify three mimicry epitopes, one each from adenine nucleotide translocator 1 (ANT), sarcoplasmic/endoplasmic reticulum Ca^{2+} ATPase 2a (SERCA2a) and cardiac troponin I. None of these induced cross-reactive T cell responses. Next, we generated major histocompatibility complex (MHC) class II dextramers to enumerate the frequencies of antigen-specific T cells to determine whether T cells with multiple antigen specificities are generated by CVB3 infection. These analyses revealed appearance of CD4 T cells positive for SERCA2a $971-990$, and cardiac myosin heavy chain-α (Myhc) $334-352$ dextramers, both in the periphery and also in the hearts of CVB3-infected animals. While ANT $21-40$ dextramer$^+$ T cells were inconsistently detected, the β1-adrenergic receptor $181-200/211-230$ or branched chain α-ketoacid dehydrogenase kinase $111-130$ dextramer$^+$ cells were absent. Interestingly, SERCA2a $971-990$, Myhc $334-352$ and ANT $21-40$ dextramer$^+$ cells were also detected in the liver indicating that they may have a pathogenic role. Finally, we demonstrate that the SERCA2a $971-990$-reactive T cells generated in CVB3 infection could transfer disease to naïve mice. The data suggest that CVB3 infection can lead to the generation of autoreactive T cells for multiple antigens indicating a possibility that the autoreactive T cells localized in the liver can potentially circulate and contribute to the development of viral myocarditis.

1. Introduction

Myocarditis can occur in association with a wide spectrum of infectious agents, systemic diseases, and hypersensitivity to drugs and toxins (Fung et al., 2016; Pollack et al., 2015). The virus-induced myocarditis in neonates and children may lead to fulminant myocarditis (Rose, 2016), and affected individuals can develop chronic myocarditis leading to dilated cardiomyopathy (DCM) and congestive heart failure. Approximately, half of these patients undergo heart transplantation due to the lack of effective treatment options (Caforio et al., 2013; Chi et al., 2014). Enteroviruses like Coxsackievirus B (CVB)3 and adenoviruses are generally suspected as causes of viral myocarditis in North America and Europe, respectively (Blauwet and Cooper, 2010; Lasrado et al., 2020), and virus-reactive antibodies, and viral RNA have been detected in up to 50–70% of those affected, suggesting that CVB3 may be an important trigger in the DCM pathogenesis (Baboonian and McKenna, 2003; Cihakova and Rose, 2008; Fujinami et al., 2006; Kuhl et al., 2005). Autoimmunity is one possible mechanism as DCM patients can carry autoantibodies for cardiac myosin heavy chain-α (Myhc), adenine nucleotide translocator 1 (ANT), β1-adrenergic receptor (β1AR), branched chain α-ketoacid dehydrogenase (BCKD), sarcoplasmic/endoplasmic reticulum Ca^{2+} ATPase 2a (SERCA2a) and cardiac troponin I (TNI) (Caforio et al., 2001; Caforio et al., 2002; Kaya et al., 2012). But, the role of autoreactive T cells, if any remains to be investigated.

Mouse models are commonly employed to determine the mechanisms of immune pathogenesis of CVB infection. CVB3 infections in susceptible mouse strains such as A/J and BALB/c are characterized by two phases that occur in continuum namely, acute myocarditis/viral phase and chronic myocarditis/non-viral phase (Cihakova and Rose, 2008; Rabausch-Starz et al., 1994; Rose et al., 1986). Affected animals show antibodies for various cardiac and non-cardiac proteins such as cardiac myosin, ANT, β1AR, BCKD, SERCA2a, TNI, laminin and muscarinic receptor, suggesting a role for autoreactive T cells in the generation of autoantibodies (Caforio et al., 2005; Fairweather et al., 2012; Kaya et al., 2012). We recently demonstrated that A/J mice infected with CVB3 show Myhc 334−352-specific CD4 T cells that are pathogenic in nature (Gangaplara et al., 2012), indicating that autoreactive T cells with multiple antigen-specificities could be generated as a secondary event in infected animals. By addressing the molecular mimicry hypothesis, we found no evidence for appearance of cross-reactive T cells to ANT, SERCA2a and TNI that had sequences mimicking CVB3 proteins. However, by analyzing the frequencies of antigen-specific T cells using major histocompatibility complex (MHC) class II dextramers for five different autoantigens, we detected the presence of T cells positive for SERCA2a 971−990 and Myhc 334−352 dextramers both in the periphery and also in the infected hearts. Interestingly, dextramer (dext⁺) T cells for select antigens were also detected in the livers suggesting a possibility that these cells can potentially circulate and contribute to viral myocarditis in infected animals.

2. Materials and methods

2.1. Mice

A/J (H-2ᵃ, male and female, 6–8 weeks old) and SJL/J (H-2ˢ, female, 4–6 weeks old) mice were procured from the Jackson Laboratory (Bar Harbor, ME), and maintained by the institutional guidelines at the University of Nebraska-Lincoln. Euthanasia was performed using a carbon dioxide chamber according to the Panel on Euthanasia, the American Veterinary Medical Association.

2.2. Virus propagation, titration, and disease-induction

Vero cells (ATCC, Manassas, VA) were used to grow CVB3 (Nancy strain, ATCC) as described previously (Gangaplara et al., 2012). After confirming the cytopathic effect (CPE), tissue culture infective dose (TCID)$_{50}$ values were determined according to the Spearman-Karber method (Reed and Muench, 1938), and the viral stocks were stored at −80 °C. To infect mice, virus diluted in 1× phosphate-buffered saline (PBS) to a final concentration of 50–2000 TCID$_{50}$/200 μL was administered intraperitoneally. Animals were housed in filter-top cages that were changed once in 3 days until termination. Clinically, animals were inspected daily for ruffled fur, isolation, sluggish activity or mortalities. At termination (days, 18–21 post-infection), lymphoid (spleen and lymph nodes) and non-lymphoid organs (hearts, pancreata and livers) were collected for histology and *in vitro* experimentation.

2.3. Peptide synthesis

Myhc 334−352 (DSAFDVLSFTAEEKAGVYK), ANT 21−40 (VSKTAVAPIERVKLLLQVQH), β1AR 181−200 (TVWAISALVSFLPILMHWWR)/211−230 (NDPKCCDFVTNRAYAIASSV), BCKDk 111−130 (PIKDQADEAQYCQLVRQLLD), SERCA2a 971−990 (KISLPVILMDETLKFVARNY), bovine ribonuclease (RNase 43−56) (VNTFVHESLADVQA), proteolipid protein (PLP) 139−151 (HSLGKWLGHPDKF), human immunodeficiency virus glycoprotein 120 (HIV) P18-I10 (Neopeptide, Cambridge, MA), and moth cytochrome C (MCC) 82−103 (FAGLKKANERADLIAYLKQATK) (GenScript, Piscataway, NJ), including the peptides listed in the Table S1 were synthesized by 9-fluorenylmethyloxycarbonyl chemistry (Neopeptide). The purity of peptides was confirmed to be more than 90 % by high-performance liquid chromatography, and their identities were confirmed by mass spectroscopy. Peptides were dissolved in ultra-pure water or PBS and stored at −20 °C.

2.4. Immunization procedures

Peptide emulsions were prepared in complete Freund's adjuvant (CFA) containing *Mycobacterium tuberculosis* H37RA extract (Difco Laboratories, Detroit, MI) to a final concentration of 5 mg/mL, except that PLP 139–151 was prepared at 1 mg/mL (Miller and Karpus, 2007; Reddy et al., 2003). A/J mice were immunized twice subcutaneously in inguinal and sternal regions on days 0 and 7 (Basavalingappa et al., 2016; Donermeyer et al., 1995; Massilamany et al., 2011d), whereas SJL/J mice received a single dose of PLP 139–151 emulsion (Miller and Karpus, 2007; Reddy et al., 2003).

2.5. Proliferation assay

Lymphocyte suspensions were prepared from a pool of spleens and lymph nodes harvested from CVB3-infected mice after lysing the erythrocytes using 1× ammonium chloride potassium buffer (Lonza, Walkersville, MD). Likewise, lymph node cells (LNCs) were prepared from immunized animals. After washing, cell pellets were suspended in RPMI containing 10 % FBS, 1 mM sodium pyruvate, 4 mM L-glutamine, 1× each of non-essential amino acids and vitamin mixture, and 100 U/mL penicillin-streptomycin (Lonza; hereafter called growth medium). Cells were stimulated with the indicated peptides (0−100 μg/mL) for 2 days in growth medium at a density of 5×10^6 cells/mL in triplicates, whereas cells cultured with no peptides were used as medium controls. After pulsing with tritiated ³[H] thymidine (1 μCi per well; MP Biomedicals, Santa Ana, CA) for 16 h, proliferative responses were measured as counts per minute (cpm) using a Wallac liquid scintillation counter (Perkin Elmer, Waltham, MA) (Basavalingappa et al., 2016; Massilamany et al., 2016). In some experiments, for easy depiction, stimulation indices were calculated by dividing the cpm values obtained in peptide-stimulated cultures by the values obtained in medium controls.

2.6. Creation of MHC dextramer and tetramer reagents

Our studies involved the use of MHC class II dextramers for both IAᵏ and/or IEᵏ alleles, and also MHC class I tetramers for H-2Dᵈ allele (Table 1). Essentially, dextramers and tetramers were created as we have reported previously (Massilamany et al., 2016; Massilamany et al., 2011a;

Table 1
The list of dextramers/tetramers used to analyze antigen-specific T cells in mice infected with CVB3.

MHC class II dextramers	
IA^k	IE^k
Myhc 334 − 352	β_1AR 181 − 200
ANT 21 − 40	SERCA2a 971 − 990
β_1AR 211 − 230	MCC 82 − 103 (control)
BCKDk 111 − 130	
SERCA2a 971 − 990	
RNase 43 − 56 (control)	

MHC class I tetramers (H-2D^d)
Myhc 338 − 348
HIV P18-I10 (control)

Myhc, cardiac myosin heavy chain-α.
ANT, adenine nucleotide translocator 1.
β_1AR, β1-adrenergic receptor.
BCKDk, branched chain α-ketoacid dehydrogenase kinase.
SERCA2a, sarcoplasmic/endoplasmic reticulum Ca^{2+} ATPase.
RNase, bovine ribonuclease.
MCC, moth cytochrome C.
HIV, human immunodeficiency virus.

Massilamany et al., 2011c; Reddy et al., 2003). We had described the creation of all dextramers and tetramers (Basavalingappa et al., 2017; Krishnan et al., 2017; Krishnan et al., 2018; Massilamany et al., 2016; Massilamany et al., 2011c) except, IA^k dextramers for ANT 21 − 40. To generate ANT 21 − 40 dextramers, the nucleotide sequence of ANT 21 − 40 (gtctccaagacggcggtcgccccgatcgagagggtcaaactgctgctgcaggtccagcat) was assembled to IA^k-β construct, and after expressing the IA^k-α and IA^k-β constructs in the Baculovirus using sf9 insect cells, soluble IA^k/ANT 21 − 40 MHC monomers were purified using the antibody affinity column (clone, 10 − 2.16) and the proteins were biotinylated. Dextramerization was performed by mixing biotinylated protein and streptavidin-fluorophore-conjugated dextran molecules at a ratio of 20:1 to obtain fluorophore-assembled dextramers as we have described earlier (Massilamany et al., 2011c; Reddy et al., 2003). In experiments involving SJL mice, we used IA^s dextramers for PLP 139–151 and Theiler's murine encephalomyelitis virus (TMEV) 70–86 as reported previously (Massilamany et al., 2014a; Massilamany et al., 2011c).

2.7. Isolation of mononuclear cells from liver and heart tissues

After euthanasia, animals were perfused by injecting 10 mL of ice-cold PBS into the left ventricles, and hearts and livers were collected to isolate mononuclear cells (MNCs) as reported previously (Gangaplara et al., 2012; Krishnan et al., 2017). In brief, livers were minced, and the dissociated tissues were treated with Collagenase IV (400 U/mL; Worthington, Lakewood, NJ) and DNase I (150 U/mL; Worthington) at 37 ˚C in shaker incubator for 30 min. After washing, MNCs were harvested using 40 %/75 % percoll gradient centrifugation procedure as described previously (Krishnan et al., 2017). After lysing erythrocytes, cell pellets were dissolved for further experimentation. For isolation of MNCs from hearts, the minced tissues were treated with Collagenase II (600 U/mL; Worthington Biochemical Corporation, Lakewood, NJ, USA) and DNase I (60 U/mL; AppliChem GmbH, Darmstadt, Germany) for 30 min at 37 ˚C using tube rotator (Miltenyi Biotec Inc., Auburn, CA). Cell suspensions were filtered through 70 μM cell strainer, and after removing the residual debris using debris removal kit (Miltenyi Biotec) and lysing erythrocytes, MNC suspensions were obtained.

2.8. Dextramer and tetramer staining

Lymphocytes harvested from mice infected with or without CVB3 were stimulated with peptides for two days, and growth medium

supplemented with interleukin (IL)-2 [IL-2 medium] was then added. Cells were stained with IA^k/IE^k dextramers during days 8–10 post-stimulation, followed by staining with anti-CD4 (GK1.5, Biolegend, San Diego, CA) and 7-aminoactinomycin-D (7-AAD) as we have described previously (Krishnan et al., 2017, 2018; Massilamany et al., 2011c). Finally, cells were washed and acquired by flow cytometry and the frequencies of dext$^+$ CD4$^+$ T cells were enumerated within the live cells (7-AAD$^-$) using FlowJo software (Tree Star, Ashland, OR). This protocol was also used to stain LNC cultures prepared from SJL mice immunized with PLP 139–151 as described previously (Massilamany et al., 2011c). The MNCs harvested from hearts and livers from CVB3-infected and liver MNCs from PLP 139–151 immunized animals were directly stained *ex vivo* as above (Krishnan et al., 2017; Massilamany et al., 2011c).

For staining with H-2D^d/MHC class I tetramers, cells were initially treated with 10 % mouse serum and Fc blocker (Biolegend), followed by staining with anti-CD4, anti-CD8a (KT15 and CT-CD8a, Invitrogen, Carlsbad, CA) and 7-AAD on ice for 15 min. Staining was continued for an additional 15 min on ice after adding H-2D^d/MHC class I tetramers, where tetramers prepared at a ratio of 8:1 between biotinylated H-2D^d/ Myhc 338 − 348 and streptavidin at a concentration of 30 μg/mL were previously optimized in pilot studies. After series of washes, cells were acquired by flow cytometry and the percentage of tetramer (tet)$^+$ CD8$^+$ cells were analyzed using FlowJo software (Tree Star).

2.9. Adoptive transfer experiments

Lymphocytes were harvested from A/J mice infected with CVB3 and cells were stimulated with SERCA2a 971 − 990 (20 μg/mL) for two days and IL-2 medium was then supplemented. On day 7 or 8, cells were expanded by treating with Concanavalin A (Con A, 2.5 μg/mL, 2 days). Viable cells harvested on day 9 or 10 post stimulation were administered to naïve A/J mice (3.0–4.0 × 10^7 cells/animal) intravenously that were primed with LPS on day -4 and day 0 (25 μg/animal) (Basavalingappa et al., 2016; Hamada et al., 2004; Massilamany et al., 2016). Each animal also received pertussis toxin (PT, 100 ng; List Biologicals, Campbell, CA) on day 0 and 2 post-transfer (Agarwal et al., 2002; Fujimoto et al., 2006; Massilamany et al., 2011d). Animals were euthanized on day 14, post-transfer, and hearts and pancreata were examined by a Board-Certified, pathologist blinded to treatment groups for inflammatory changes by hematoxylin and eosin (H & E) staining as described previously (Basavalingappa et al., 2016; Krishnan et al., 2017; Massilamany et al., 2011d). In some experiments, heart and pancreatic sections obtained from mice infected with or without CVB3 were also examined by H & E staining as above.

2.10. Detection of CVB3 RNA

Total RNA was extracted from hearts and pancreata tissues harvested from naïve A/J mice using the Trizol method (Invitrogen) and to remove genomic DNA, 1 μg of total RNA was treated with amplification grade DNase I (Invitrogen). cDNAs were synthesized using iScript™ reverse transcription supermix kit, as recommended (Bio-Rad, Hercules, CA). PCR amplifications were performed using CVB3 viral protein (VP) 1-specific primers (forward, 5′-TTGCATATGGCCCAGTGGAAG-3′; reverse, 5′-TGTGGATCCTTATTGCCTAGTAGTGGTAACTC-3′) and glyceraldehyde-3-phosphate dehydrogenase (GAPDH) primers (forward, 5′-CGGCAAATTCAACGGCACAGTCAA-3′; reverse, 5′-CTTTCCAGAGGG GCCATCCACAG-3′) (Basavalingappa et al., 2016; Gangaplara et al., 2012). The PCR products were stained with ethidium bromide and resolved on 1.5 % agarose gel electrophoresis.

2.11. Statistics

Right-tailed paired Wilcoxon signed rank test was used to compare frequencies of dext$^+$ cells in splenocytes derived from CVB3-infected animals (Wilcoxon, 1945). The corresponding controls used for

comparison include: RNase $43-56$ for IA^k dextramers (Myhc $334-352$, ANT $21-40$ and BCKDk $111-130$), combined RNase $43-56$ and MCC $82-103$ for IA^k and IE^k dextramers (SERCA2a $971-990$ and β$_1$AR $211-230/$ $181-200$), and MCC $82-103$ for β$_1$AR $181-200$. For comparing frequencies of dext$^+$ cells in liver and heart MNCs, right-tailed non-parametric Wilcoxon rank sum test was used (Mann and Whitney, 1947). Student's *t*-test was used to determine differences in the frequencies of CD4$^+$ dext$^+$ T cells between infected and non-infected (naïve) mice, ANT $21-40$ dext$^+$ cells in immunized animals, and also to analyze Myhc $338-348$ tet$^+$CD8$^+$ T cells.

3. Results

3.1. Identification of mimicry epitopes from CVB3 proteome that have a potential to induce cross-reactive immune responses

By using LALIGN tool (Madeira et al., 2019), we sought to analyze CVB3 proteome to identify myocarditogenic mimicry epitopes by aligning CVB3 sequence with six self-antigens that are commonly implicated as autoantigens in patients with myocarditis/DCM. These include, Myhc, ANT, β$_1$AR, BCKDk, SERCA2a and TNI (Caforio et al., 2001; Caforio et al., 2002; Kaya et al., 2012). The expectation was that the mimicry peptides can result in the generation of cross-reactive T cells due to T cell degeneracy (Gautam et al., 1998; Wooldridge et al., 2012). These analyses led us to identify a panel of 29 mimics representing ANT, β$_1$AR, BCKDk, SERCA2a and TNI, and their percent similarities were, 35–43%, 30–47%, 33–40%, 32–46% and 28–47% respectively (Table S1). However, such a degree of sequence similarity was lacking for Myhc (data not shown). We also noted that the mimicry epitopes were found localized in both structural (VP1 to VP4) and non-structural regions (2B, 2C, 3C protease and 3D polymerase) of CVB3 genome. The structural proteins of viruses are generally considered as immunogenic, and VP1, is one such protein identified in many enteroviruses, including CVB3, TMEV, and poliovirus (Huber et al., 1993; Minor et al., 1986; Yauch and Kim, 1994). Similarly, several examples of both self-[ribonuclease (RNase), glucose-6-phosphate isomerase, and glutamate decarboxylase] (Atkinson et al., 1994; Basu et al., 2000; Kaufman et al., 1992; Lorenz et al., 1988) and foreign-antigens (neuraminidase and rhodanese-related sulfur transferase) (Massilamany et al., 2010, Massilamany et al., 2011b; Schaeffer et al., 1989) also exist to predict that the non-structural proteins can be immunogenic.

3.2. Analysis of T cell responses to self-peptides that mimic CVB3 proteins in A/J mice infected with CVB3

From a panel of 29 mimicry peptides, we tested a hypothesis that the CVB3 infection can lead to the induction of cross-reactive T cell responses for self-antigens listed in the Table S1. To test this hypothesis, we used 24 peptides representing the ANT, β$_1$AR, BCKDk, SERCA2a and TNI, and the remaining five peptides could not be synthesized. After infecting A/J mice with CVB3, lymphocytes prepared on day 21 post-infection were used in ^{3}[H]-thymidine-incorporation assay to measure proliferative responses. By using RNase $43-56$ as control, T cell responses were noted for three peptides namely, ANT 33–49, SERCA2a 799–813 and TNI 138–159 to be ∼1.4-fold difference (Fig. S1). Although their magnitude was marginal, occurrence of T cell responses selectively to 3 out of 24 peptides may mean that the CVB3 mimicry epitopes might be immunogenic in the infected animals. But, this proposition required additional validation.

3.3. Evaluation of cross-reactive T cell responses induced by CVB3 mimicry epitopes in immunized animals

To further evaluate if mimicry epitopes can induce cross-reactive T cell responses, we utilized an immunization protocol to determine the immunogenicity of three peptide pairs in crisscross experiments. These

include, ANT 33–49/CVB 1153–1169, SERCA2a 799–813/CVB 1839–1853 and TNI 138–159/CVB 1527–1548. Of note, the CVB sequences listed above are conserved in all the six serotypes of CVB (Table S2), leading to a prediction that exposure to any CVB serotype can potentially induce cross-reactive T cell responses. In the first setting, A/J mice were immunized with self-peptides (ANT 33–49, SERCA2a 799–813 and TNI 138–159), and T cell reactivity was tested to both immunizing peptides and also their mimicry epitopes, CVB 1153–1169, CVB 1839–1853 and CVB 1527–1548. The analysis revealed T cell responses occurring only to one pair (ANT 33–49/CVB 1153–1169), and responses were lacking for two other pairs (Fig. S2a). Similar analysis in the second setting that involved immunization with CVB3 mimics revealed marginal responses to two CVB3 epitopes namely, CVB 1153–1169, and CVB 1839–1853 (Fig. S2b). However, cross-reactive responses for their corresponding mimics from self-antigens were lacking (ANT 33–49, and SERCA2a 799–813). We had expected that the T cells sensitized with CVB 1153–1169 respond to its mimic, ANT 33–49, since ANT 33–49-sensitized T cells did respond to CVB 1153–1169 in a crisscross experiment as described above (Fig. S2a, left panel). Since the CVB mimics did not result in cross-reactive T cell responses in the immunization settings that involved the use of CFA as a potent, immune-stimulating adjuvant, we concluded that CVB3 infection is unlikely to lead to the induction of significant cross-reactive T cell responses to be biologically significant. However, a possibility exists that cross-reactivity can occur for other autoantigens. For example, by searching the structural databases using the crystal structure of ANT (PDB ID: 1OKC) (Pebay-Peyroula et al., 2003), we found a peptide fragment within the LOTUS domain of the meiosis regulator and mRNA stability factor 1 (MARF1) (PDB ID: 5YAD), an orthologue of human Limkain B (LMKB) (Yao et al., 2018). As shown in the Fig. S3, top panel, comparison of sequences between ANT 33–49 and CVB 1153–1169 revealed an identity of 35.3 %, and in a similar comparison between MARF1 and CVB 1153–1169, the identity was found to be 41.2 %. Furthermore, using the structures of ANT and MARF1, we predicted the helical structural model for CVB 1153–1169 to be similar as well (Fig. S3, bottom panel). Importantly, LMKB/MARF1 appears to act as an autoantigen that may have a role in the regulation of inflammatory response (Bloch et al., 2014; Dunster et al., 2005), but we have not investigated these possibilities. However, it is also to be noted that ANT contains multiple immunodominant epitopes, and we had demonstrated that one epitope, ANT $21-40$ can induce myocarditis in A/J mice by generating autoreactive T cells (Basavalingappa et al., 2016). We reasoned that detection of ANT 33–49-reactive T cells in CVB3-infected animals might have represented a *de novo* population as a result of cardiac damage induced by the virus, since 47 % of residues (8/17) are similar between the two epitopes (ANT 33–49, <u>K</u>LLL<u>QVQH</u>ASK<u>QISAEK</u>; and ANT $21-40$ VSKTAVAPIERV<u>KLLLQVQH</u>, similar residues are underlined).

3.4. Derivation of MHC dextramers to analyze antigen-specific, autoreactive T cells in CVB3-infected mice

By using MHC dextramers (Fig S4a), we addressed a hypothesis that CVB3 infection can lead to the generation of autoreactive T cells with multiple antigen-specificities, and our previous work with the demonstration of Myhc-reactive T cells in CVB3-infected animals also supported this proposition (Gangaplara et al., 2012). We targeted a total of five autoantigens namely, Myhc, ANT, β$_1$AR, BCKDk and SERCA2a, and we and others had previously characterized the myocarditis-inducing, immunodominant epitopes in all of these antigens (Basavalingappa et al., 2016; Basavalingappa et al., 2017; Daniels et al., 2008; Krishnan et al., 2017; Krishnan et al., 2018; Massilamany et al., 2011d). We also had reported creation and validation of MHC class II dextramers for Myhc, β$_1$AR, BCKDk and SERCA2a (Table 1). These include IA^k dextramers for Myhc $334-352$ (Massilamany et al., 2011c), BCKDk $111-130$ (Krishnan et al., 2017), SERCA2a $971-990$ (Krishnan et al., 2018) and β$_1$AR $211-230$ (Basavalingappa et al., 2017), and also IE^k dextramers for SERCA2a $971-990$ (Krishnan et al., 2018) and β$_1$AR

$181 - 200$ (Basavalingappa et al., 2017). The reason to create IA^k and IE^k dextramers is that SERCA2a $971 - 990$ was found to bind both IA^k and IE^k MHC class II alleles (Krishnan et al., 2018), whereas β_1AR has two epitopes, with one epitope each, binding to IA^k (β_1AR $211 - 230$) or IE^k molecule (β_1AR $181 - 200$) (Basavalingappa et al., 2017). To define specificity, we used two control dextramers with one each, for IA^k (RNase $43 - 56$), and IE^k allele (MCC $82 - 103$). In this report, we have described the generation of dextramers for ANT $21 - 40$ and validated using LNCs obtained from ANT $21 - 40$-immunized animals by flow cytometry (Fig. S4b). The analysis revealed that ANT $21 - 40$ dextramers bind CD4 T cells antigen-specifically, since staining for control dextramers was negligible (ANT $21 - 40$: 2.02 ± 0.66 vs 0.33 ± 0.03 %, P = 0.043; Fig S4b). We thus, generated a panel of seven dextramers to evaluate the detection of antigen-specific, CD4 T cells in CVB3-infected animals (Table 1).

3.5. CVB3 infection leads to the generation of autoreactive T cells with multiple antigen-specificities

Groups of A/J mice were infected with CVB3, and lymphocytes harvested approximately 20 days post-infection were stimulated with or without Myhc $334 - 352$, ANT $21 - 40$, BCKDk $111 - 130$, SERCA2a $971 - 990$, β_1AR $181 - 200$, and β_1AR $211 - 230$, and dextramer staining was performed during 8–10 days post-stimulations as illustrated in the Fig. S5. The flow cytometric analysis revealed detection of Myhc $334 - 352$ dext$^+$ CD4$^+$ T cells to be higher than the control (RNase $43 - 56$) as expected (0.41 ± 0.11 vs 0.18 ± 0.03 %, p = 0.031) (Fig. 1). Similarly, by analyzing the SERCA2a $971 - 990$-reactive T cells using IA^k and IE^k dextramers, we noted significant increase (five-fold) in their frequencies as compared to RNase $43 - 56$/MCC $82 - 103$ controls (1.28 ± 0.42 vs 0.24 ± 0.04 %, p = 0.00098) (Fig. 1). Although, similar trends were noted for ANT $21 - 40$ dextramers relative to control (0.56 ± 0.14 vs 0.21 ± 0.05 %), no significant differences were noted for other dextramers namely, BCKDk $111 - 130$ (0.26 ± 0.03 vs 0.17 ± 0.02 %), and β_1AR $211 - 230$ or β_1AR $181 - 200$ (0.37 ± 0.15 vs 0.25 ± 0.07 %). We also analyzed the frequencies of cells positive for Myhc $334 - 352$ (0.26 ± 0.03 vs 0.41 ± 0.11, p = 0.03) and SERCA2a $971 - 990$ (0.31 ± 0.05 vs 1.28 ± 0.42, p = 0.05) dextramers to be higher in infected mice as compared to naïve animals (Fig S6). Thus, detection of dext$^+$ T cells only for two from a panel of five antigens suggest that they may have a role in the CVB3 pathogenesis.

3.6. Autoreactive T cells can infiltrate into the livers of CVB3-infected mice

In addressing a hypothesis that the T cells specific to promiscuously-expressed antigens can infiltrate various organs, we had previously demonstrated the detection of BCKDk $111 - 130$-specific T cells in the livers from animals immunized with BCKDk $111 - 130$ (Krishnan et al., 2017). Thus, we expected that the BCKDk-reactive T cells may infiltrate livers in CVB3-infected animals. We isolated the liver MNCs from CVB3-infected animals and performed dextramer staining using BCKDk $111 - 130$ dextramers as shown in the Fig. S7. The analysis revealed no significant differences in the number of BCKDk $111 - 130$ dext$^+$ T cells as compared to control (RNase $43 - 56$) (0.85 % vs 0.27 %, p = 0.083) (Fig. 2). We then extended this observation to determine whether autoreactive T cells specific to other autoantigens can be detected in the livers of CVB3-infected animals by taking advantage of the availability of other dextramers (IA^k dextramers: Myhc $334 - 352$ and ANT $21 - 40$; IA^k and IE^k dextramers: SERCA2a $971 - 990$; and IE^k dextramers: β_1AR $181 - 200$) (Table 1). These analyses revealed detection of significant number of CD4 T cells positive for Myhc $334 - 352$ (1.36 % vs 0.27 %, p = 0.003), ANT $21 - 40$ (1.44 % vs 0.27 %, p = 0.0003) and SERCA2a $971 - 990$ (1.30 % vs 0.22 %, p = 0.009), but not β_1AR $181 - 200$ dextramers (0.49 % vs 0.29 %) as compared to their corresponding controls (Fig. 2). The data suggest that detection of autoreactive T cells

in the liver might not have occurred as a random event. We made this proposition since liver MNCs obtained from animals immunized with an irrelevant antigen, PLP 139–151 in SJL mice did not reveal T cells positive for PLP 139–151 dextramers (Fig. S8, top panel), in spite of their presence in the LNCs (Fig. S8, bottom panel). However, we needed to address whether the autoreactive T cells generated in CVB3-infected animals can infiltrate the target organ, heart.

3.7. Heart infiltrates from CVB3-infected animals show detection of autoreactive CD4 and CD8 T cells

In our previous study, we had demonstrated the detection of Myhc-reactive T cells in hearts from CVB3-infected animals (Gangaplara et al., 2012). Since, the current study revealed appearance of SERCA2a $971 - 990$ dext$^+$ T cells, but to a lesser degree for ANT $21 - 40$ dextramers, we asked if SERCA2a $971 - 990$-reactive T cells can infiltrate hearts in infected animals. We performed dextramer staining on MNCs from hearts harvested from CVB3-infected animals using Myhc $334 - 352$, ANT $21 - 40$ and SERCA2a $971 - 990$ dextramers as shown in the Fig. S7. The analysis revealed detection of CD4$^+$ T cells staining with Myhc $334 - 352$ (1.01 % vs 0.37 %, p = 0.021) and SERCA2a $971 - 990$ (1.07 % vs 0.46 %, p = 0.0027), but not ANT $21 - 40$ dextramers (1.23 % vs 0.37 %, p = 0.279) when compared with their controls (Fig. 3). Furthermore, we had previously noted that the heart infiltrates from CVB3-infected animals contain both CD4 and CD8 T cells (Gangaplara et al., 2012). In addition, we also had demonstrated that the Myhc $334 - 352$ encompasses epitopes for both CD4 and CD8 T cells (Massilamany et al., 2016). Since, we noted the detection of Myhc $334 - 352$ dext$^+$ CD4$^+$ T cells in the hearts from CVB3-infected mice, we asked whether CD8 T cells specific to Myhc $338 - 348$ could be detected in the hearts from CVB3-infected animals. To this end, we created MHC class I/H-2D^d tetramers for Myhc $338 - 348$. By using HIV P18-I10 tetramers as controls, we detected the Myhc $338 - 348$ tet$^+$ CD8$^+$ T cells in significant frequencies in splenocytes from CVB3-infected animals (0.4 % vs 0.02 %, p = 0.015) (Fig. 4a, top panel), but such a frequency was low in non-infected animals (Fig. S9). We also noted significant number of CD8 T cells binding to Myhc $338 - 348$ tetramers in the heart MNCs as compared to control tetramers (4.0 % vs 0.38 %, p = 0.005) (Fig. 4b, bottom panel). The data suggest that the Myhc-reactive CD8 T cells infiltrating the hearts may also contribute to cardiac damage.

3.8. Autoreactive T cells generated in CVB3-infected mice are pathogenic in nature

To determine the pathogenicity of autoreactive T cell responses generated in CVB3-infected mice, we used adoptive transfer protocol with an expectation that the autoreactive T cells can transfer disease to naïve animals as we had previously demonstrated for Myhc $334 - 352$ (Gangaplara et al., 2012). In this study, we tested the pathogenic potential of SERCA2a $971 - 990$-reactive T cells generated in CVB3-infected mice. As shown in the Fig. 5, top left [atrium, (i), and myocardium of ventricle, (ii)] and their corresponding insets in the middle panels (ia, and iia), we noted that the naïve mice receiving T cells sensitized with SERCA2a $971 - 990$ had infiltrations in the epicardium and myocardium with the lesions being apparent in the atria as compared to ventricles. However, pancreatic sections from these animals did not reveal any inflammatory changes (Fig. 5, top right panel), indicating that the disease-inducing ability of SERCA2a $971 - 990$-sensitized T cells was limited to heart. Similarly, heart, and pancreatic sections from control groups (saline and LPS/PT) (Fig. 5, bottom panel) and also those from uninfused naïve mice (Fig. S10, top panel) had no pathological changes as expected. Furthermore, by comparing the heart and pancreatic inflammatory changes in CVB3-infected mice with the recipients of SERCA2a $971 - 990$-reactive T cells, we noted that sections from CVB3-infected mice had a widespread inflammatory foci
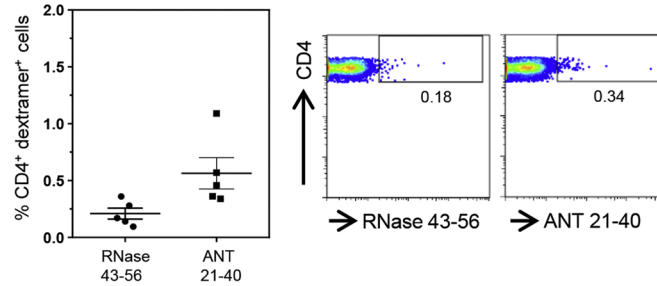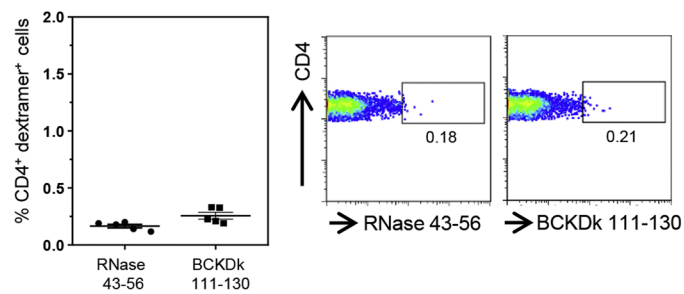
IA^k/Myhc 334-352 dextramers
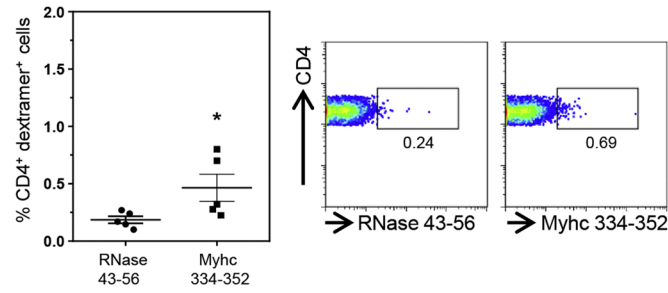
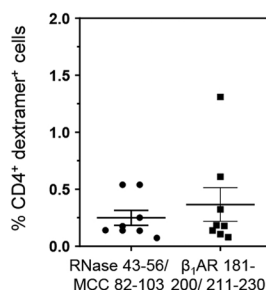## IA^k/SERCA2a 971-990 dextramers   IE^k/SERCA2a 971-990 dextramers
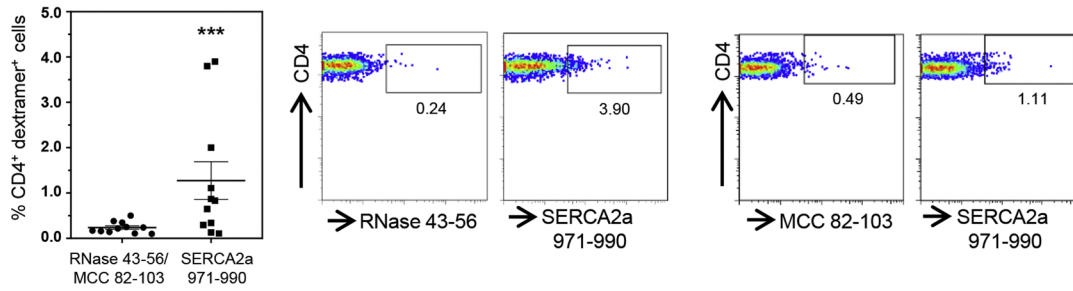
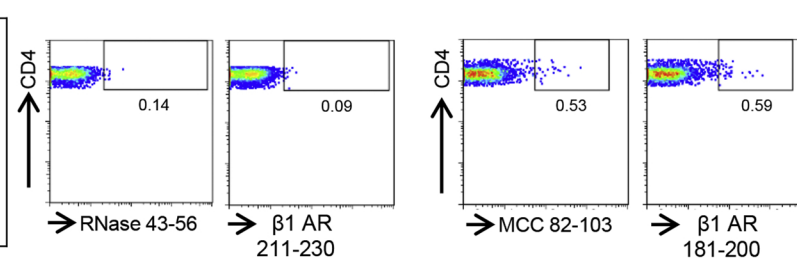## IA^k/ANT 21-40 dextramers

IA^k/BCKDk 111-130 dextramers

IA^k/β$_1$AR 211-230 dextramers   IE^k/β$_1$AR 181-200 dextramers

(caption on next page)

Fig. 1. Detection of autoreactive T cells with multiple antigen-specificities in animals infected with CVB3. Lymphocytes obtained from animals infected with CVB3 were stimulated with Myhc 334-352, SERCA2a 971-990, ANT 21-40, BCKDk 111-130, and β_1AR 181-200 or β_1AR 211-230 for three days, and cells were rested in IL-2 medium. Cells harvested on day 8 to 10 post-stimulation were stained with the indicated IA^k and/or IE^k dextramers, anti-CD4 and 7-AAD. After washing, and acquiring by flow cytometry, dext$^+$ CD4$^+$ cells were enumerated. Mean ± SEM values obtained from three to six individual experiments, each involving three to six mice are indicated in the left panel for each dextramer reagent. Representative flow cytometric plots for control and specific dextramers are shown on the right. RNase 43-56, control for IA^k dextramers; and MCC 82-103, control for IE^k dextramers. *P < 0.05 and ***P < 0.001.

accompanied with necrosis and mineralization in both hearts and pancreas (Fig. S10, bottom panel). As reported previously, such a diffused nature is expected in infected animals that reflects damage resulting from both cytolytic properties of virus and immune response (Gangaplara et al., 2012; Garmaroudi et al., 2015; C. Massilamany et al., 2014b). We then sought to rule out a possibility of residual viral nucleic acid, if any in the cell suspensions used for adoptive transfer experiments. We performed RT-PCR analysis on the RNA samples prepared from hearts and pancreata harvested from the recipients of saline or cells to detect the presence of viral RNA using primers specific to CVB3 VP1 (Fig. 6). The PCR analysis revealed no amplifications for VP1 suggesting that the inflammatory changes noted in the hearts from animals that received SERCA2a 971−990-reactive T cells are not due to residual virus. Taken together, our data provide evidence that CVB3 infection can result in the generation of pathogenic autoreactive T cells with specificities for multiple antigens supporting the notion that pathogens primarily affecting the target organs can secondarily result in the generation of pathogenic autoimmune responses.

4. Discussion

In this report, we have described the characterization of autoreactive T cells, including cross-reactive T cell responses in viral myocarditis induced with CVB3. Previous reports indicate that antibodies and T cells specific to streptococcal M protein could cross-react with cardiac myosin, suggesting that cross-reactive T cells can contribute to the pathogenesis of rheumatic heart disease (Dale and Beachey, 1985; Pruksakorn et al., 1994). Additionally, while antibodies for ANT and CVB3 could cross-react with each other (Schwimmbeck et al., 1993),

antibodies generated against one self-antigen, namely cardiac myosin could cross-react with another self-antigen β_1AR, potentially leading to apoptosis of cardiomyocytes, thus supporting a role for antibodies in the CVB pathogenesis (Li et al., 2006). However, it was unknown whether pathogenic cross-reactive T cells can be generated in CVB3 infection for antigens that are commonly implicated as autoimmune targets in DCM patients. These include cardiac (Myhc, TNI, β_1AR and SERCA2a) and/or non-cardiac (ANT and BCKDk) antigens (Caforio et al., 2001; Caforio et al., 2002; Kaya et al., 2012; Neumann et al., 1991). We identified three mimicry epitopes, CVB 1153–1169, CVB 1839–1853 and CVB 1527–1548, respectively for ANT 33–49, SERCA2a 799–813 and TNI 138–159. However, by analyzing their cross-reactive T cell responses in the immunization settings, none of them induced significant responses except that T cell reactivity was more apparent for ANT 33–49 than others, raising questions as to the relevance of molecular mimicry hypothesis in the causation of CVB3 myocarditis. First, the finding that lack of detection of cross-reactive T cells for antigens tested in our studies suggests that they do not contribute to the initiation and progression of myocarditis induced with CVB3. However, a possibility exists that the antibodies generated against these antigens may still be relevant to CVB3 pathogenesis. In support of this notion, immune complexes have been demonstrated for ANT and BCKDk in the serum from CVB3-infected animals (Neumann et al., 1994), but their pathogenic role remains unclear. Likewise, our data also do not rule out a possibility for appearance of cross-reactive T cells for other antigens that were not investigated in our studies. One such potential antigen that we have identified is LMKB/MARF1 (Dunster et al., 2005). In these scenarios however, pathogenicity of cross-reactive T cells needs to be demonstrated in adoptive transfer experiments to provide a proof-of
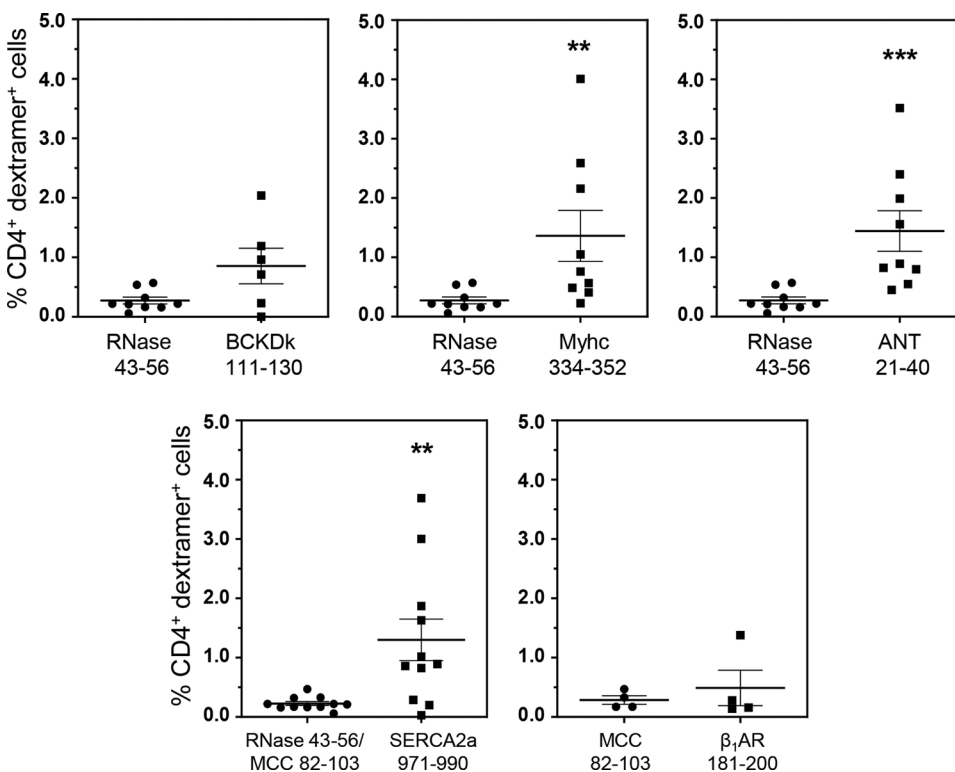

Fig. 2. Detection of autoreactive T cells in the livers from CVB3-infected mice. Livers from CVB3-infected mice were processed to obtain MNCs as described in the methods section. MNCs were stained with the indicated IA^k and/or IE^k dextramers, followed by anti-CD4, and 7-AAD. After acquiring the cells by flow cytometry, dext$^+$ cells were analyzed in the live (7-AAD$^-$), CD4 subset. Mean ± SEM values from four to nine individual experiments, each involving three to six mice are shown. RNase 43-56 (control for IA^k dextramers); and MCC 82-103 (control for IE^k dextramers). **P < 0.01, and ***P < 0.001.
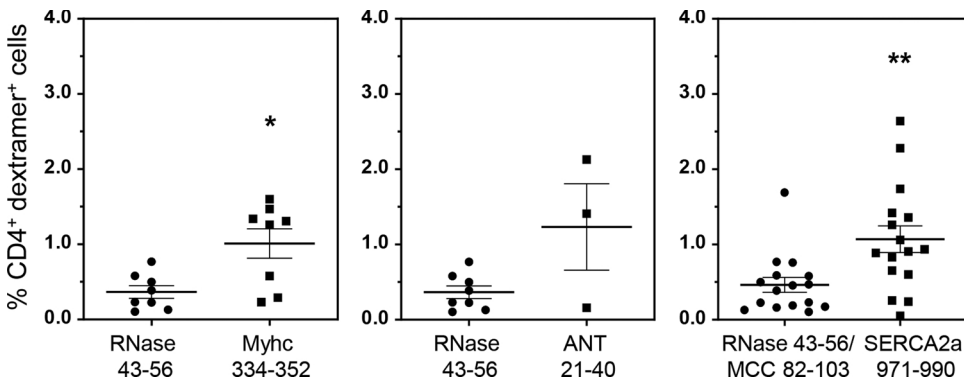
Fig. 3. Heart infiltrates from CVB3-infected mice revealed the presence of SERCA2a 971-990 dext[+] CD4 T cells. After perfusing the CVB3-infected animals at termination, hearts were collected and processed to obtain MNCs as described in the Methods section. Cells were then stained with the indicated dextramers, anti-CD4 and 7-AAD. After acquiring by flow cytometry, the frequencies of dext^{+} CD4^{+} T cells were determined. The data sets represent mean ± SEM values derived from three to eight experiments each involving three to six mice. Controls, RNase 43-56 for IA[k] dextramers and MCC 82-103 for IE[k] dextramers. *P < 0.05 and **P < 0.01.

concept that they are biologically relevant to CVB3 pathogenesis. Second, antibody cross-reactivity has been noted between ANT, actin, β_1AR and myosin with CVB3 (Cunningham et al., 1992; Maisch et al., 1993; Mascaro-Blanco et al., 2008; Schulze and Schultheiss, 1995) that can also potentially result from formation of anti-idiotypic antibodies (Root-Bernstein and Fairweather, 2015). However, direct evidence is lacking as to the pathogenic role of such cross-reactive antibodies in CVB3 myocarditis. Nevertheless, it is possible that cross-reactive antibodies may indirectly contribute to viral pathogenesis as demonstrated with cardiac myosin and β_1AR as described above (Li et al., 2006; Mascaro-Blanco et al., 2008).

We next investigated whether CVB3 infection can lead to the generation of autoreactive T cells with multiple antigen-specificities, since we had previously reported that CVB3 infection can result in the induction of pathogenic Myhc-reactive CD4 T cells (Gangaplara et al., 2012). We analyzed the frequencies of antigen-specific, CD4 T cells using a panel of seven MHC class II dextramers, and the analyses revealed detection of Myhc $334-352$ dext^{+} CD4^{+} T cells as expected (Gangaplara et al., 2012). In addition, CD4 T cells positive for SERCA2a $971-990$ dextramers also were detected in the splenocytes from CVB3-infected animals. These data reinforce the notion that the cardio tropic pathogens like CVB3 can cause damage to the myocardium leading to

release of intracellular antigens such as Myhc and SERCA2a that can later become immunogenic in infected animals. Lack of detection of significant proportions of T cells for ANT $21-40$, β_1AR $181-200/211-230$ and BCKDk $111-130$ dextramers may imply that these antigens might not be released in CVB3 infection or these antigenic determinants might not have been naturally presented in the infected animals.

We had previously made an observation that CD4 T cells sensitized with BCKDk $111-130$ could induce both autoimmune hepatitis and myocarditis in A/J mice immunized with BCKDk $111-130$ (Krishnan et al., 2017). We had proposed that BCKDk may be an autoimmune target for induction of hepatitis because its expression can occur in the liver (Muller and Danner, 2004). Additionally, CVB3 can also infect liver (Liu et al., 2013). Therefore, we performed dextramer analysis using the liver infiltrates in CVB3-infected animals leading to the detection of T cells positive for SERCA2a $971-990$, Myhc $334-352$ and ANT $21-40$ dextramers, but not for other antigens. Detection of ANT $21-40$-reactive T cells in the liver was not expected as T cells positive for ANT $21-40$ dextramers were not significantly elevated in the splenocytes. Previous reports suggest that antigen-sensitized CD8 T cells, including autoreactive T cells, can migrate to liver and die by apoptosis (Crispe et al., 2000; Park et al., 2002). Although, we do not
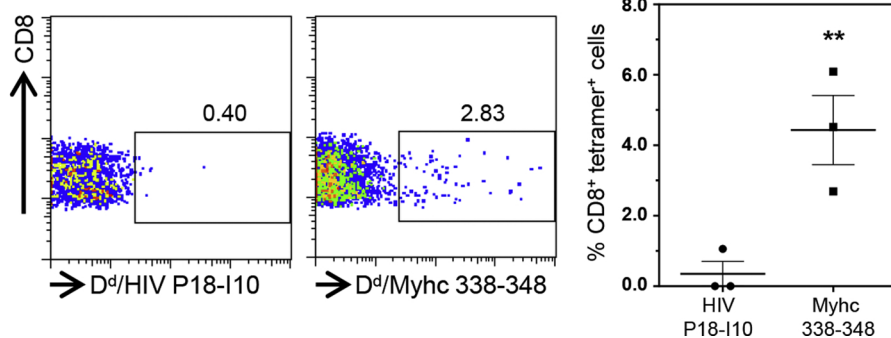
a. Splenocytes
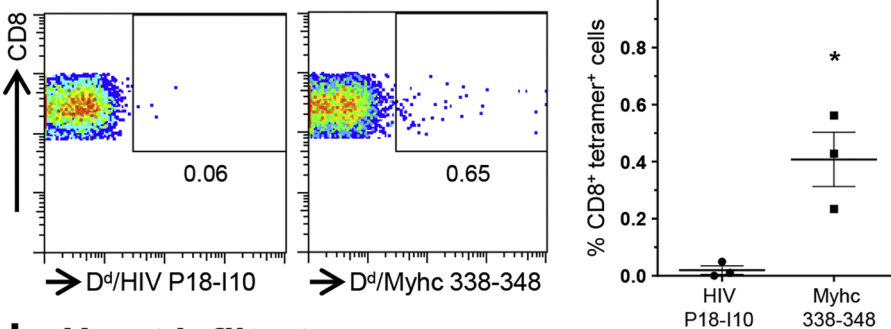
b. Heart infiltrates

Fig. 4. CVB3 infection leads to the generation of Myhc 338-348 tet^{+} CD8^{+} T cells. (a) Splenocytes. Between 18 to 21 days post-infection with CVB3, splenocytes were prepared and stimulated with Myhc 334-352 for three days. After resting in IL-2 medium, cells harvested on day 8 or 9 were stained with CD4 and CD8 antibodies and 7-AAD and H-2D[d]/Myhc 338-348 (specific) and HIV P18-I10 (control) tetramers. Cells were washed and acquired by flow cytometry to determine the frequencies of tet^{+} cells in the live (7-AAD[−]) CD8 subset. (b) Heart infiltrates. Hearts collected from CVB3-infected animals were processed to obtain MNCs. Cells were stained as above, and after acquiring by flow cytometry, frequencies of live (7-AAD^{−}), tet^{+} CD8^{+} cells were enumerated. Representative flow cytometric plots and mean ± SEM values derived from four experiments each involving two to three mice are shown. *P < 0.05 and **P < 0.01.
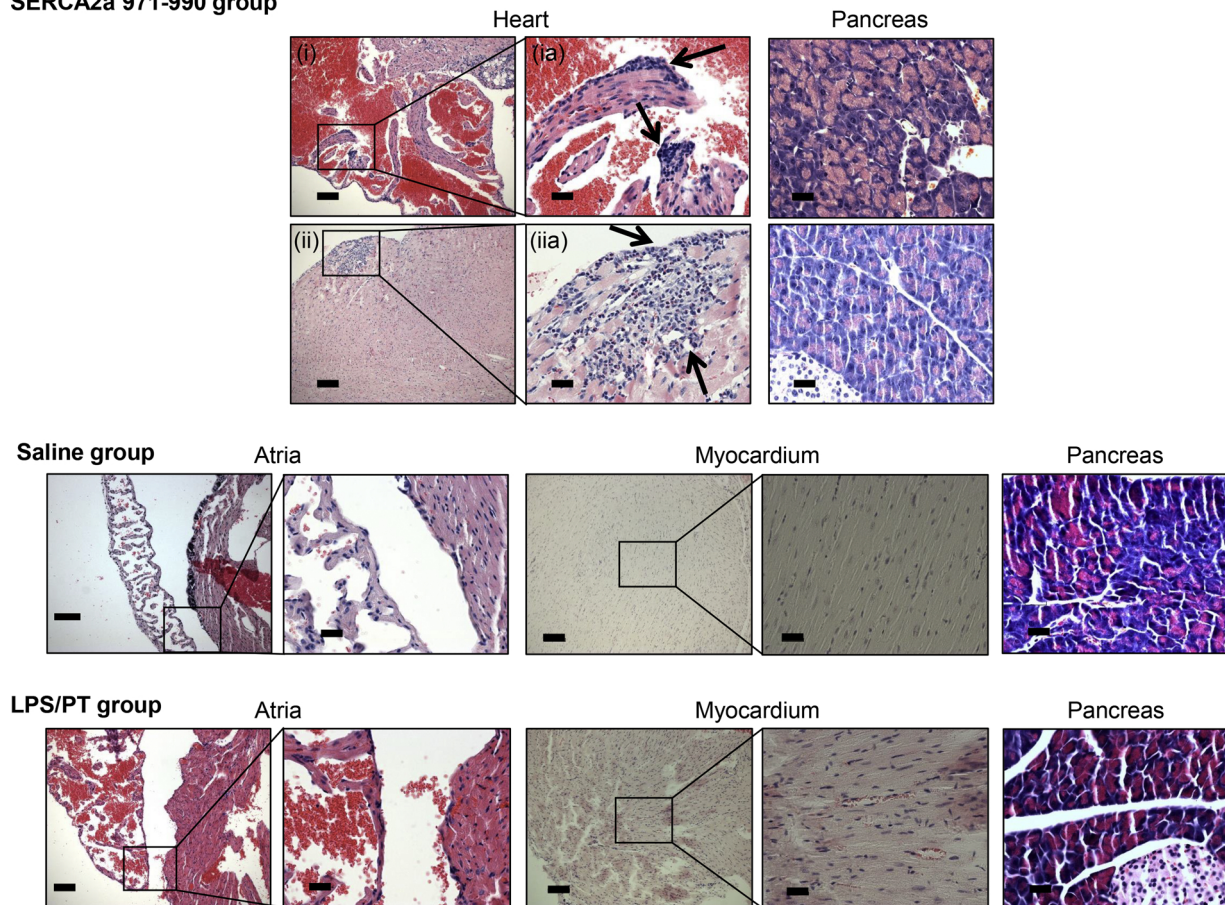
SERCA2a 971-990 group

Fig. 5. SERCA2a-reactive T cells from CVB3-infected mice can induce myocarditis in naïve A/J mice. Splenocytes were obtained from animals infected with CVB3 between 10 to 21 days post-infection, and the cells were stimulated with SERCA2a 971-990 for two days. After resting in IL-2 medium, SERCA2a-specific cells were expanded with Con-A and the viable cells were administered into naïve A/J mice that were primed with LPS and PT as described in the methods section, where, saline-recipients and LPS/PT-primed animals uninfused with cells were used as controls. At termination on day 14 post-transfer, hearts and pancreata were collected for histological evaluation by H and E staining. Sections in the top panel represent animals that received SERCA2a 971-990-reactive T cells, where infiltrations were noted in the atria (i, and inset, ia) and myocardium (ii, and inset, iia) are shown with arrows. The bottom panel represents sections from saline and LPS/PT-groups. Normal pancreatic sections are shown in the right panels in all the groups. Representative sections from groups of four animals are shown.

discount the possibility that the autoreactive T cells being detected in our studies may represent those that are destined to die, additional studies are needed to determine as to why only SERCA2a, Myhc and ANT-reactive CD4 T cells were selectively detected in the liver. It is also possible that SERCA2a $971-990$ and ANT $21-40$-sensitized T cells can cross-react with their isoforms, SERCA2b and ANT-2, respectively, whose expression can also occur in the liver (Arai et al., 1992; Levy et al., 2000). Importantly, whether autoreactive T cells localized in the liver can recirculate in infected animals also need detailed analysis. Likewise, although CD4 T cell exhaustion is poorly understood as compared to CD8 T cells (Saeidi et al., 2018), whether the autoreactive $CD4^+$ T cells that we have observed in our studies possess exhaustion phenotype may be worth investigating in the future. However, since liver can be affected in CVB3 infection (Liu et al., 2013), autoreactive T cells localized in the liver may have a pathogenic role in CVB3 infection.

Finally, to determine the pathogenic significance of autoreactive T cells in the causation of myocarditis, we performed dextramer staining analysis on heart infiltrates and the analysis revealed the presence of CD4 T cells positive for SERCA2a $971-990$ and Myhc $334-352$ dextramers. Since, Myhc $334-352$ was found to harbor a CD8 T cell determinant (Myhc $338-348$) (Massilamany et al., 2016), we used MHC class I tetramers (H-2D^d) for Myhc $338-348$. We demonstrate that the heart infiltrates from CVB3-infected animals contain Myhc $338-348$

tet$^+$ CD8$^+$ T cells suggesting that Myhc-reactive CD8 T cells may contribute to the disease pathogenesis. In support of this proposition, we had previously demonstrated that the CD8 T cells generated in response to Myhc $334-352$-immunization, induced myocarditis in naïve mice in adoptive transfer experiments (Massilamany et al., 2016). In this study, we demonstrate that the SERCA2a $971-990$-reactive T cells generated in CVB3-infected animals are pathogenic as indicated by their ability to transfer myocarditis to naïve mice with the inflammatory lesions being frequently detected in the atria. This was an expected phenotype because A/J mice immunized with SERCA2a $971-990$ develop mainly atrial myocarditis (Krishnan et al., 2018) that can be attributed to abundant expression of SERCA2a in the atria as compared to ventricles (Lüss et al., 1999).

In summary, by testing the molecular mimicry hypothesis, we did not observe cross-reactive T cells for autoantigens tested in our studies. Whether CVB3 infection can lead to the generation of cross-reactive T cells for other antigens needs further investigations. Such a possibility exists for LMKB/MARF1 as described above (Dunster et al., 2005). Conversely, our data support a possibility that CVB3 infection can lead to the generation of pathogenic autoreactive T cells with multiple antigen specificities. We envision that a combination of virus-induced damage to cardiomyocytes due to cytolytic properties of CVB3, and inflammatory damage induced by the host response may lead to the release of various intracellular and surface antigens including cryptic
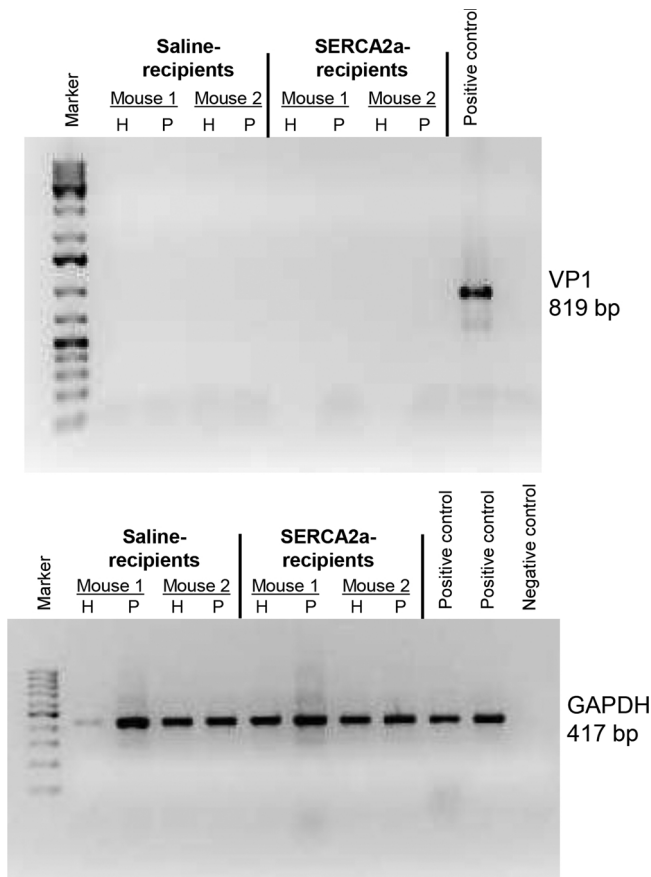
Fig. 6. Evaluation of CVB3 RNA in mice that received SERCA2a 971-990–re-active T cells. Total RNA was extracted from hearts and pancreata representing the indicated groups with two animals in each, and the cDNAs derived from these samples were evaluated for the presence of CVB3 VP1 (top panel) and GAPDH (housekeeping gene) by PCR using the sequence-specific primers. The PCR products analyzed by ethidium bromide in the agarose (1.5%) gel elec-trophoresis are shown. VP1 PCR product, positive control; water without template, negative control.

epitopes, and trigger the generation of autoreactive T cells, which in turn can infiltrate hearts and aggravate inflammation. Such a repertoire of cells can also be generated consequent to engulfment of dying car-diomyocytes resulting from virus-induced apoptosis (Esfandiarei and McManus, 2008) and autophagy (Garmaroudi et al., 2015) processes. A proportion of these autoreactive T cells may remain dormant with a possibility that their activation may occur through bystander activation up on exposure to non-specific infections, and they may contribute to the development of chronic myocarditis/DCM in CVB3-infected ani-mals. Since T cells occupy a central role in the induction of auto-immunity, and their help is critical for B cells to produce antibodies, T cells may be the main mediators of cardiac autoimmunity in CVB3 in-fection.

Author contributions

R.H.B., R.A., N.L. and J.R. conceived and designed the experiments; R.H.B., R.A., N.L., B.Y., C.M. and A.G. performed the experiments; R.H.B., N.L., J.-J.R., S.H.X. and D.S. analyzed the data; and R.H.B., R.A., N.L., S.H.X and J.R wrote the manuscript.

Declaration of Competing Interest

The authors declare no competing interests.

References

Agarwal, R.K., Sun, S.H., Su, S.B., Chan, C.C., Caspi, R.R., 2002. Pertussis toxin alters the innate and the adaptive immune responses in a pertussis-dependent model of auto-immunity. J. Neuroimmunol. 129, 133–140.
Arai, M., Otsu, K., Maclennan, D.H., Periasamy, M., 1992. Regulation of sarcoplasmic reticulum gene expression during cardiac and skeletal muscle development. Am. J. Physiol.-Cell Physiol. 262, C614–C620.
Atkinson, M.A., Bowman, M.A., Campbell, L., Darrow, B.L., Kaufman, D.L., Maclaren, N.K., 1994. Cellular immunity to a determinant common to glutamate decarboxylase and coxsackie virus in insulin-dependent diabetes. J. Clin. Invest. 94, 2125–2129.
Baboonian, C., McKenna, W., 2003. Eradication of viral myocarditis: is there hope? J. Am. Coll. Cardiol. 42, 473–476.
Basavalingappa, R.H., Massilamany, C., Krishnan, B., Gangaplara, A., Kang, G., Khalilzad-Sharghi, V., Han, Z., Othman, S., Li, Q., Riethoven, J.-J., 2016. Identification of an epitope from Adenine nucleotide translocator 1 that induces inflammation in heart in A/J mice. Am. J. Pathol. 186, 3160–3175.
Basavalingappa, R.H., Massilamany, C., Krishnan, B., Gangaplara, A., Rajasekaran, R.A., Afzal, M.Z., Riethoven, J.J., Strande, J.L., Steffen, D., Reddy, J., 2017. Beta1-Adrenergic Receptor Contains Multiple IA(k) and IE(k) Binding Epitopes That Induce T Cell Responses with Varying Degrees of Autoimmune Myocarditis in A/J Mice. Front. Immunol. 8, 1567.
Basu, D., Horvath, S., Matsumoto, I., Fremont, D.H., Allen, P.M., 2000. Molecular basis for recognition of an arthritic peptide and a foreign epitope on distinct MHC molecules by a single TCR. J. Immunol. 164, 5788–5796.
Blauwet, L.A., Cooper, L.T., 2010. Myocarditis. Prog. Cardiovasc. Dis. 52, 274–288.
Bloch, D.B., Li, P., Bloch, E.G., Berenson, D.F., Galdos, R.L., Arora, P., Malhotra, R., Wu, C., Yang, W., 2014. LMKB/MARF1 localizes to mRNA processing bodies, interacts with Ge-1, and regulates IFI44L gene expression. PLoS One 9, e94784.
Caforio, A.L., Mahon, N.J., McKenna, W.J., 2001. Cardiac autoantibodies to myosin and other heart-specific autoantigens in myocarditis and dilated cardiomyopathy. Autoimmunity 34, 199–204.
Caforio, A.L., Mahon, N.J., Tona, F., McKenna, W.J., 2002. Circulating cardiac auto-antibodies in dilated cardiomyopathy and myocarditis: pathogenetic and clinical significance. Eur. J. Heart Fail. 4, 411–417.
Caforio, A.L., Daliento, L., Angelini, A., Bottaro, S., Vinci, A., Dequal, G., Tona, F., Iliceto, S., Thiene, G., McKenna, W.J., 2005. Autoimmune myocarditis and dilated cardio-myopathy: focus on cardiac autoantibodies. Lupus 14, 652–655.
Caforio, A.L., Pankuweit, S., Arbustini, E., Basso, C., Gimeno-Blanes, J., Felix, S.B., Fu, M., Heliö, T., Heymans, S., Jahns, R., 2013. Current state of knowledge on aetiology, diagnosis, management, and therapy of myocarditis: a position statement of the European Society of Cardiology Working Group on Myocardial and Pericardial Diseases. Eur. Heart J. 34, 2636–2648.
Chi, N.-H., Chou, N.-K., Yu, Y.-H., Yu, H.-Y., Wu, I.-H., Chen, Y.-S., Huang, S.-C., Ko, W.-J., Wang, S.-S., 2014. Heart transplantation in endstage rheumatic heart disease. Circ. J. 78, 1900–1907.
Cihakova, D., Rose, N.R., 2008. Pathogenesis of myocarditis and dilated cardiomyopathy. Adv. Immunol. 99, 95–114.
Crispe, I.N., Dao, T., Klugewitz, K., Mehal, W.Z., Metz, D.P., 2000. The liver as a site of T-cell apoptosis: graveyard, or killing field? Immunol. Rev. 174, 47–62.
Cunningham, M.W., Antone, S.M., Gulizia, J.M., McManus, B.M., Fischetti, V.A., Gauntt, C.J., 1992. Cytotoxic and viral neutralizing antibodies crossreact with streptococcal M protein, enteroviruses, and human cardiac myosin. Proc. Natl. Acad. Sci. U. S. A. 89, 1320–1324.
Dale, J.B., Beachey, E.H., 1985. Epitopes of streptococcal M proteins shared with cardiac myosin. J. Exp. Med. 162, 583–591.
Daniels, M.D., Hyland, K.V., Wang, K., Engman, D.M., 2008. Recombinant cardiac myosin fragment induces experimental autoimmune myocarditis via activation of Th1 and Th17 immunity. Autoimmunity 41, 490–499.
Donermeyer, D.L., Beisel, K.W., Allen, P.M., Smith, S.C., 1995. Myocarditis-inducing epitope of myosin binds constitutively and stably to I-Ak on antigen-presenting cells in the heart. J. Exp. Med. 182, 1291–1300.
Dunster, K., Lai, F.P., Sentry, J.W., 2005. Limkain b1, a novel human autoantigen loca-lized to a subset of ABCD3 and PXF marked peroxisomes. Clin. Exp. Immunol. 140, 556–563.
Esfandiarei, M., McManus, B.M., 2008. Molecular biology and pathogenesis of viral myocarditis. Annu. Rev. Pathol. 3, 127–155.
Fairweather, D., Stafford, K.A., Sung, Y.K., 2012. Update on coxsackievirus B3 myo-carditis. Curr. Opin. Rheumatol. 24, 401–407.
Fujimoto, C., Yu, C.R., Shi, G., Vistica, B.P., Wawrousek, E.F., Klinman, D.M., Chan, C.C., Egwuagu, C.E., Gery, I., 2006. Pertussis toxin is superior to TLR ligands in enhancing pathogenic autoimmunity, targeted at a neo-self antigen, by triggering robust ex-pansion of Th1 cells and their cytokine production. J. Immunol. 177, 6896–6903.

Fujinami, R.S., Von Herrath, M.G., Christen, U., Whitton, J.L., 2006. Molecular mimicry, bystander activation, or viral persistence: infections and autoimmune disease. Clin. Microbiol. Rev. 19, 80–94.

Fung, G., Luo, H., Qiu, Y., Yang, D., McManus, B., 2016. Myocarditis. Circ. Res. 118, 496–514.

Gangaplara, A., Massilamany, C., Brown, D.M., Delhon, G., Pattnaik, A.K., Chapman, N., Rose, N., Steffen, D., Reddy, J., 2012. Coxsackievirus B3 infection leads to the generation of cardiac myosin heavy chain-α-reactive CD4 T cells in A/J mice. Clin. Immunol. 144, 237–249.

Garmaroudi, F.S., Marchant, D., Hendry, R., Luo, H., Yang, D., Ye, X., Shi, J., McManus, B.M., 2015. Coxsackievirus B3 replication and pathogenesis. Future Microbiol. 10, 629–653.

Gautam, A.M., Liblau, R., Chelvanayagam, G., Steinman, L., Boston, T., 1998. A viral peptide with limited homology to a self peptide can induce clinical signs of experimental autoimmune encephalomyelitis. J. Immunol. 161, 60–64.

Hamada, Y., Takata, M., Kiyoku, H., Enzan, H., Doi, Y., Fujimoto, S., 2004. Monomethoxypolyethylene glycol-modified cardiac myosin treatment blocks the active and passive induction of experimental autoimmune myocarditis. Circ. J. 68, 149–155.

Huber, S., Polgar, J., Moraska, A., Cunningham, M., Schwimmbeck, P., Schultheiss, P., 1993. T lymphocyte responses in CVB3-induced murine myocarditis. Scand. J. Infect. Dis. Suppl. 88, 67–78.

Kaufman, D.L., Erlander, M.G., Clare-Salzler, M., Atkinson, M.A., Maclaren, N.K., Tobin, A.J., 1992. Autoimmunity to two forms of glutamate decarboxylase in insulin-dependent diabetes mellitus. J. Clin. Invest. 89, 283–292.

Kaya, Z., Leib, C., Katus, H.A., 2012. Autoantibodies in heart failure and cardiac dysfunction. Circ. Res. 110, 145–158.

Krishnan, B., Massilamany, C., Basavalingappa, R.H., Gangaplara, A., Kang, G., Li, Q., Uzal, F.A., Strande, J.L., Delhon, G.A., Riethoven, J.J., 2017. Branched chain α-ketoacid dehydrogenase kinase 111–130, a T cell epitope that induces both autoimmune myocarditis and hepatitis in A/J mice. Immun. Inflamm. Dis.

Krishnan, B., Massilamany, C., Basavalingappa, R.H., Gangaplara, A., Rajasekaran, R.A., Afzal, M.Z., Khalilzad-Sharghi, V., Zhou, Y., Riethoven, J.J., Nandi, S.S., Mishra, P.K., Sobel, R.A., Strande, J.L., Steffen, D., Reddy, J., 2018. Epitope mapping of SERCA2a identifies an antigenic determinant that induces mainly atrial myocarditis in A/J mice. J. Immunol. 200, 523–537.

Kuhl, U., Pauschinger, M., Noutsias, M., Seeberg, B., Bock, T., Lassner, D., Poller, W., Kandolf, R., Schultheiss, H.P., 2005. High prevalence of viral genomes and multiple viral infections in the myocardium of adults with "idiopathic" left ventricular dysfunction. Circulation 111, 887–893.

Lasrado, N., Yalaka, B., Reddy, J., 2020. Triggers of inflammatory heart disease. Front. Cell Dev. Biol. 8.

Levy, S.E., Chen, Y.S., Graham, B.H., Wallace, D.C., 2000. Expression and sequence analysis of the mouse adenine nucleotide translocase 1 and 2 genes. Gene 254, 57–66.

Li, Y., Heuser, J.S., Cunningham, L.C., Kosanke, S.D., Cunningham, M.W., 2006. Mimicry and antibody-mediated cell signaling in autoimmune myocarditis. J. Immunol. 177, 8234–8240.

Liu, J.Y., Wang, S.M., Chen, I.C., Yu, C.K., Liu, C.C., 2013. Hepatic damage caused by coxsackievirus B3 is dependent on age-related tissue tropisms associated with the coxsackievirus-adenovirus receptor. Pathog. Dis. 68, 52–60.

Lorenz, R.G., Tyler, A.N., Allen, P.M., 1988. T cell recognition of bovine ribonuclease. Self/non-self discrimination at the level of binding to the I-Ak molecule. J. Immunol. 141, 4124–4128.

Lüss, I., Boknik, P., Jones, L.R., Kirchhefer, U., Knapp, J., Linck, B., Lüss, H., Meissner, A., Müller, F.U., Schmitz, W., 1999. Expression of cardiac calcium regulatory proteins in atrium v ventricle in different species. J. Mol. Cell. Cardiol. 31, 1299–1314.

Madeira, F., Park, Y.M., Lee, J., Buso, N., Gur, T., Madhusoodanan, N., Basutkar, P., Tivey, A.R.N., Potter, S.C., Finn, R.D., Lopez, R., 2019. The EMBL-EBI search and sequence analysis tools APIs in 2019. Nucleic Acids Res. 47, W636–W641.

Maisch, B., Bauer, E., Cirsi, M., Kochsiek, K., 1993. Cytolytic cross-reactive antibodies directed against the cardiac membrane and viral proteins in coxsackievirus B3 and B4 myocarditis. Characterization and pathogenetic relevance. Circulation 87 IV49-65.

Mann, H.B., Whitney, D.R., 1947. On a test of whether one of two random variables is stochastically larger than the other. Ann. Math. Statist. 18, 50–60.

Mascaro-Blanco, A., Alvarez, K., Yu, X., Lindenfeld, J., Olansky, L., Lyons, T., Duvall, D., Heuser, J.S., Gosmanova, A., Rubenstein, C.J., Cooper, L.T., Kem, D.C., Cunningham, M.W., 2008. Consequences of unlocking the cardiac myosin molecule in human myocarditis and cardiomyopathies. Autoimmunity 41, 442–453.

Massilamany, C., Steffen, D., Reddy, J., 2010. An epitope from Acanthamoeba castellanii that cross-react with proteolipid protein 139-151-reactive T cells induces autoimmune encephalomyelitis in SJL mice. J. Neuroimmunol. 219, 17–24.

Massilamany, C., Gangaplara, A., Chapman, N., Rose, N., Reddy, J., 2011a. Detection of cardiac myosin heavy chain-alpha-specific CD4 cells by using MHC class II/IA(k) tetramers in A/J mice. J. Immunol. Methods 372, 107–118.

Massilamany, C., Thulasingam, S., Steffen, D., Reddy, J., 2011b. Gender differences in CNS autoimmunity induced by mimicry epitope for PLP 139-151 in SJL mice. J. Neuroimmunol. 230, 95–104.

Massilamany, C., Upadhyaya, B., Gangaplara, A., Kuszynski, C., Reddy, J., 2011c.

Detection of autoreactive CD4 T cells using major histocompatibility complex class II dextramers. BMC Immunol. 12, 40.

Massilamany, C., Gangaplara, A., Steffen, D., Reddy, J., 2011d. Identification of novel mimicry epitopes for cardiac myosin heavy chain-α that induce autoimmune myocarditis in A/J mice. Cell. Immunol. 271, 438–449.

Massilamany, C., Gangaplara, A., Jia, T., Elowsky, C., Li, Q., Zhou, Y., Reddy, J., 2014a. In situ detection of autoreactive CD4 T cells in brain and heart using major histocompatibility complex class II dextramers. J. Vis. Exp., e51679.

Massilamany, C., Gangaplara, A., Reddy, J., 2014b. Intricacies of cardiac damage in coxsackievirus B3 infection: implications for therapy. Int. J. Cardiol. 177, 330–339.

Massilamany, C., Gangaplara, A., Basavalingappa, R.H., Rajasekaran, R.A., Khalilzad-Sharghi, V., Han, Z., Othman, S., Steffen, D., Reddy, J., 2016. Localization of CD8 T cell epitope within cardiac myosin heavy chain-α 334–352 that induces autoimmune myocarditis in A/J mice. Int. J. Cardiol. 202, 311–321.

Miller, S.D., Karpus, W.J., 2007. Experimental autoimmune encephalomyelitis in the mouse. Curr. Protoc. Immunol Chapter 15, Unit 15 11.

Minor, P.D., Ferguson, M., Evans, D.M., Almond, J.W., Icenogle, J.P., 1986. Antigenic structure of polioviruses of serotypes 1, 2 and 3. J. Gen. Virol. 67 (Pt 7), 1283–1291.

Muller, E.A., Danner, D.J., 2004. Tissue-specific translation of murine branched-chain α-ketoacid dehydrogenase kinase mRNA is dependent upon an upstream open reading frame in the 5′-untranslated region. J. Biol. Chem. 279, 44645–44655.

Neumann, D.A., Lane, J.R., LaFond-Walker, A., Allen, G.S., Wulff, S.M., Herskowitz, A., Rose, N.R., 1991. Heart-specific autoantibodies can be eluted from the hearts of Coxsackievirus B3-infected mice. Clin. Exp. Immunol. 86, 405–412.

Neumann, D., Rose, N., Ansari, A., Herskowitz, A., 1994. Induction of multiple heart autoantibodies in mice with coxsackievirus B3-and cardiac myosin-induced autoimmune myocarditis. J. Immunol. 152, 343–350.

Park, S., Murray, D., John, B., Crispe, I.N., 2002. Biology and significance of T-cell apoptosis in the liver. Immunol. Cell Biol. 80, 74–83.

Pebay-Peyroula, E., Dahout-Gonzalez, C., Kahn, R., Trezeguet, V., Lauquin, G.J., Brandolin, G., 2003. Structure of mitochondrial ADP/ATP carrier in complex with carboxyatractyloside. Nature 426, 39–44.

Pollack, A., Kontorovich, A.R., Fuster, V., Dec, G.W., 2015. Viral myocarditis–diagnosis, treatment options, and current controversies. Nat. Rev. Cardiol. 12, 670–680.

Pruksakorn, S., Currie, B., Brandt, E., Phornphutkul, C., Hunsakunachai, S., Manmontri, A., Robinson, J.H., Kehoe, M.A., Galbraith, A., Good, M.F., 1994. Identification of T cell autoepitopes that cross-react with the C-terminal segment of the M protein of group A streptococci. Int. Immunol. 6, 1235–1244.

Rabausch-Starz, I., Schwaiger, A., Grunewald, K., Muller-Hermelink, H.K., Neu, N., 1994. Persistence of virus and viral genome in myocardium after coxsackievirus B3-induced murine myocarditis. Clin. Exp. Immunol. 96, 69–74.

Reddy, J., Bettelli, E., Nicholson, L., Waldner, H., Jang, M.H., Wucherpfennig, K.W., Kuchroo, V.K., 2003. Detection of autoreactive myelin proteolipid protein 139-151-specific T cells by using MHC II (IAs) tetramers. J. Immunol. 170, 870–877.

Reed, L.J., Muench, H., 1938. A simple method of estimating fifty percent endpoints. Am. J. Hyg. 27, 493–497.

Root-Bernstein, R., Fairweather, D., 2015. Unresolved issues in theories of autoimmune disease using myocarditis as a framework. J. Theor. Biol. 375, 101–123.

Rose, N.R., 2016. Viral myocarditis. Curr. Opin. Rheumatol. 28, 383–389.

Rose, N.R., Wolfgram, L.J., Herskowitz, A., Beisel, K.W., 1986. Postinfectious autoimmunity: two distinct phases of coxsackievirus B3-induced myocarditis. Ann. N. Y. Acad. Sci. 475, 146–156.

Saeidi, A., Zandi, K., Cheok, Y.Y., Saeidi, H., Wong, W.F., Lee, C.Y.Q., Cheong, H.C., Yong, Y.K., Larsson, M., Shankar, E.M., 2018. T-cell exhaustion in chronic infections: reversing the state of exhaustion and reinvigorating optimal protective immune responses. Front. Immunol. 9, 2569.

Schaeffer, E.B., Sette, A., Johnson, D.L., Bekoff, M.C., Smith, J.A., Grey, H.M., Buus, S., 1989. Relative contribution of "determinant selection" and "holes in the T-cell repertoire" to T-cell responses. Proc. Natl. Acad. Sci. U. S. A. 86, 4649–4653.

Schulze, K., Schultheiss, H.P., 1995. The role of the ADP/ATP carrier in the pathogenesis of viral heart disease. Eur. Heart J. 16 (Suppl O), 64–67.

Schwimmbeck, P.L., Schwimmbeck, N.K., Schultheiss, H.P., Strauer, B.E., 1993. Mapping of antigenic determinants of the adenine-nucleotide translocator and coxsackie B3 virus with synthetic peptides: use for the diagnosis of viral heart disease. Clin. Immunol. Immunopathol. 68, 135–140.

Wilcoxon, F., 1945. Individual comparisons by ranking methods. Biom. Bull. 1, 80–83.

Wooldridge, L., Ekeruche-Makinde, J., van den Berg, H.A., Skowera, A., Miles, J.J., Tan, M.P., Dolton, G., Clement, M., Llewellyn-Lacey, S., Price, D.A., Peakman, M., Sewell, A.K., 2012. A single autoimmune T cell receptor recognizes more than a million different peptides. J. Biol. Chem. 287, 1168–1177.

Yao, Q., Cao, G., Li, M., Wu, B., Zhang, X., Zhang, T., Guo, J., Yin, H., Shi, L., Chen, J., Yu, X., Zheng, L., Ma, J., Su, Y.Q., 2018. Ribonuclease activity of MARF1 controls oocyte RNA homeostasis and genome integrity in mice. Proc. Natl. Acad. Sci. U. S. A. 115, 11250–11255.

Yauch, R.L., Kim, B.S., 1994. A predominant viral epitope recognized by T cells from the periphery and demyelinating lesions of SJL/J mice infected with Theiler's virus is located within VP1(233-244). J. Immunol. 153, 4508–4519.